ARTICLE

BIOTECHNOLOGY and BIOENGINEERING

Amino Acid and Glucose Metabolism in Fed-Batch CHO Cell Culture Affects Antibody Production and Glycosylation

Yuzhou Fan,[1,2] Ioscani Jimenez Del Val,[3] Christian Müller,[2] Jette Wagtberg Sen,[2] Søren Kofoed Rasmussen,[2] Cleo Kontoravdi,[3] Dietmar Weilguny,[2] Mikael Rørdam Andersen[1]

[1]Network Engineering of Eukaryotic Cell Factories, Department of Systems Biology, Technical University of Denmark, Building 223, 2800 Kgs, Lyngby, Denmark; telephone: +45-45252675; fax: +45-45884148; e-mail: mr@bio.dtu.dk

[2]Symphogen A/S, Pederstrupvej 93, 2750, Ballerup, Denmark; telephone: +45-88382683; fax: +45-45265060; e-mail: dw@symphogen.com

[3]Center for Process Systems Engineering, Department of Chemical Engineering, Imperial College London, London, UK

ABSTRACT: Fed-batch Chinese hamster ovary (CHO) cell culture is the most commonly used process for IgG production in the biopharmaceutical industry. Amino acid and glucose consumption, cell growth, metabolism, antibody titer, and *N*-glycosylation patterns are always the major concerns during upstream process optimization, especially media optimization. Gaining knowledge on their interrelations could provide insight for obtaining higher immunoglobulin G (IgG) titer and better controlling glycosylation-related product quality. In this work, different fed-batch processes with two chemically defined proprietary media and feeds were studied using two IgG-producing cell lines. Our results indicate that the balance of glucose and amino acid concentration in the culture is important for cell growth, IgG titer and *N*-glycosylation. Accordingly, the ideal fate of glucose and amino acids in the culture could be mainly towards energy and recombinant product, respectively. Accumulation of by-products such as $NH4^+$ and lactate as a consequence of unbalanced nutrient supply to cell activities inhibits cell growth. The levels of Leu and Arg in the culture, which relate to cell growth and IgG productivity, need to be well controlled. Amino acids with the highest consumption rates correlate with the most abundant amino acids present in the produced IgG, and thus require sufficient availability during culture. Case-by-case analysis is necessary for understanding the effect of media and process optimization on glycosylation. We found that in certain cases the presence of Man5 glycan can be linked to limitation of UDP-GlcNAc biosynthesis as a result of insufficient extracellular Gln. However, under different culture conditions, high Man5 levels can also result from low α-1,3-mannosyl-glycoprotein 2-β-*N*-acetylglucosaminyltransferase (GnTI) and UDP-GlcNAc transporter activities, which may be attributed to high level of NH_4^+ in the cell culture. Furthermore, galactosylation of the mAb Fc glycans was found to be limited by UDP-Gal biosynthesis, which was observed to be both cell line and cultivation condition-dependent. Extracellular glucose and glutamine concentrations and uptake rates were positively correlated with intracellular UDP-Gal availability. All these findings are important for optimization of fed-batch culture for improving IgG production and directing glycosylation quality.

Biotechnol. Bioeng. 2014;9999: 1–15.

KEYWORDS: Chinese hamster ovary cells; amino acids; glucose; metabolism; fed-batch; IgG; upstream process optimization; glycosylation

Correspondence to: M. R. Andersen and D. Weilguny

Received 5 June 2014; Revision received 12 August 2014; Accepted 5 September 2014
Accepted manuscript online xx Month 2014;
Article first published online in Wiley Online Library (wileyonlinelibrary.com).
DOI 10.1002/bit.25450

Introduction

In recent decades, the annual global market of recombinant therapeutic proteins has grown significantly from ca. $12 billion in the year 2000 to $33 in 2004 and $99 billion in 2009 (Walsh, 2003, 2006, 2010). Monoclonal antibodies (mAbs), in particular, which offer novel therapy avenues for cancer, inflammatory diseases, infectious diseases, and autoimmune diseases, have had remarkable success in both regulatory approval and global sales (Jimenez Del Val et al., 2010; O'Callaghan and James, 2008). Chinese hamster ovary (CHO) cells are extensively used for the production of recombinant antibodies as a result of their robust growth and the potential to produce non-immunogenic antibodies with glycosylation patterns similar to humans (Jefferis, 2007; Raju, 2003). N-linked glycosylation plays a critical role in the biological properties of therapeutic IgG, for example, effectors function,

immunogenicity, stability, and clearance rate (Burton and Dwek, 2006; Goochee et al., 1991; Jefferis, 2009a,b; Raju, 2008). Therefore, control of glycosylation is of prime importance to meet regulatory requirements and for quality compliance. Naturally occurring IgG have two conserved *N*-glycosylation sites at Asn^{297} with the consensus sequence Asn-X-Ser/Thr on the heavy chains, where X is any amino acid except Pro. The heterogeneity of the glycan structures on each glycosylation site can vary according to their biosynthetic stage from less mature forms (e.g., non-glycosylated and high mannose forms) to more mature forms (e.g., galactosylated and sialylated forms).

The process of *N*-glycosylation, although complicated, has been well characterized (Kornfeld and Kornfeld, 1985). Initially in the endoplasmic reticulum (ER), a lipid-linked oligosaccharide precursor (Glc3Man9GlcNAc2-PP-dolichol) is synthesized by transferring *N*-acetylglucosamine, mannose, and glucose residues from UDP-GlcNAc, GDP-mannose, and UDP-glucose (the nucleotide sugars synthesized in cytosol and transported into ER), respectively, to a lipid carrier, dolichol phosphate. These precursors are subsequently transferred to the available *N*-glycosylation sequons present on the nascent polypeptide chain. The three glucose residues present on the now protein-bound oligosaccharide contribute to protein folding via the calnexin–calreticulin cycle. After the cycle has ensured adequate protein folding, all three glucose residues are cleaved from the oligosaccharide (Ellgaard and Helenius, 2003). Then, one mannose residue is trimmed in the ER prior to the IgG being translocated to the Golgi apparatus by means of vesicles (Hossler et al., 2009). In the Golgi, the N-linked glycans mature in a step-wise fashion through a number of enzyme-catalyzed reactions where monosaccharide residues are trimmed off or added to the carbohydrate structure. The maturation of glycans is largely dependent on factors such as expression, activity, and localization of the glycosidase and glycosyltransferase enzymes (Jassal et al., 2001; Kanda et al., 2006; Mori et al., 2004; Paulson and Colley, 1989; Weikert et al., 1999), the intracellular levels and availability of nucleotides and nucleotide sugars, for example, GDP-Man, UDP-GlcNAc, UDP-Glc, and UDP-Gal (Baker et al., 2001; Hills et al., 2001; Nyberg et al., 1999), and the accessibility of glycosylation sites on the glycoprotein (Holst et al., 1996). For example, the Man5 glycans can remain unprocessed due to insufficient α-mannosidase II (ManII) activity or when the GlcNAc addition reaction is limited by insufficient availability of intracellular UDP-GlcNAc or low α-1,3-mannosyl-glycoprotein 2-β-*N*-acetylglucosaminyltransferase (GnTI) activity (Pacis et al., 2011).

Glycolysis and glutaminolysis are the key metabolic pathways of CHO cells (Quek et al., 2010). Through glycolysis, CHO cells consume glucose as the main carbon source for energy production and generate lactate as the most common metabolic by-product. Glutaminolysis is the prevalent pathway through which CHO cells assimilate organic nitrogen for biomass synthesis while releasing ammonium as the main by-product (Altamirano et al., 2006; Lu et al., 2005). Fed-batch culture is widely used for the production of recombinant antibodies in industry (Huang et al., 2010). In fed-batch culture, periodic delivery of appropriate feeds provides sufficient nutrients to support cell growth and metabolism and induce a prolonged and productive culture life (Chee Furng Wong et al., 2005). However, accumulation of cellular by-products may inhibit cell growth, threaten culture longevity, reduce antibody production, and compromise antibody glycosylation (Chen and Harcum, 2005; Dorai et al., 2009; Gawlitzek et al., 2000; Hossler et al., 2009; Li et al., 2012). Understanding the interplay between cell growth, cell metabolism, IgG synthesis and glycosylation and how these factors vary among different cell lines and media composition at the metabolic level will benefit bioprocess optimization, media development and will be useful in identifying screening and engineering targets (Dean and Reddy, 2013).

Aiming at high titer production and adequate glycosylation-related quality of IgG, different strategies have been proposed to improve CHO cell culture performance. Limiting the feed of glucose (Cruz et al., 1999; Gagnon et al., 2011; Gambhir et al., 1999) and glutamine (Chee Furng Wong et al., 2005), substituting glucose (Altamirano et al., 2004, 2006) and glutamine (Altamirano et al., 2000, 2001) with alternative nutrients, addition of feed supplements (Gramer et al., 2011), optimization of process parameters such temperature, pH, agitation rate and osmolality (Ahn et al., 2008; Fox et al., 2004; Pacis et al., 2011; Senger and Karim, 2003; Trummer et al., 2006) and engineering of metabolic (Fogolin et al., 2004; Kim and Lee, 2007; Zhou et al., 2011) and anti-apoptotic (Druz et al., 2013; Mastrangelo et al., 2000) targets have all been attempted. In addition, many efforts have been made on metabolic profiling (Jimenez Del Val et al., 2011; Kochanowski et al., 2008; Sellick et al., 2011), and ^{13}C metabolic flux analysis (Ahn and Antoniewicz, 2011; Dean and Reddy, 2013; Quek et al., 2010) of CHO cell culture at different growth stages to further understand the interplay between energy, cell growth, protein production and glycosylation in CHO cells.

Herein, we present the differences in cell growth, IgG production, nutrient consumption, intracellular nucleotide sugar availability, and IgG glycosylation for two IgG-producing cell lines grown in fed-batch cultures with two different chemically-defined proprietary media and feeds. Our results provide an integrative approach to understand the relationship of glucose and amino acid metabolism, nucleotide sugar metabolism, cell growth, IgG production, and glycosylation in fed-batch CHO cell culture and give guidance for future process optimization and media development from a metabolic point of view.

Material and Methods

Cell Lines and Media

Two Symphogen in-house IgG1-producing CHO cell lines (1030 and 4384) were used in this study. Both of them were generated from a dihydrofolate reductase-deficient (DHFR-) CHO DG44 cell line (Urlaub et al., 1983) through methotrexate (MTX) mediated stable transfection with a

vector containing DHFR and the genes for antibody heavy and light chains, followed by fluorescence activated cell sorting (FACS) and adaptation to serum-free medium. All basal media and feeds used in this study are proprietary, chemically defined and serum-free. Cells were maintained and expanded in basal media B in shake flask at 200 rpm in a 37°C humidified culture incubator supplied with 5% CO_2.

Fed-Batch Culture

Cells were seeded at a density of 5×10^5 viable cells/mL for a 2-day passage or 3×10^5 viable cells/mL for a 3-day passage prior to the inoculation of fed-batch cultures. Cells in fed-batch culture were grown in 500 mL shake flasks with an initial culture volume of 70 mL at 37°C, 5% CO_2, 200 rpm. The temperature was shifted from 37 to 33.5°C on day 5. All sampling was carried out before feeding. The culture was harvested when the viability became lower than 60% or on day 14. Viability and viable cell density (VCD) was measured by Vi-CELL XR (Beckman Coulter, Brea, CA). Glucose, glutamine, lactate, ammonium, glutamate, pH, and osmolality were measured by Bioprofile 100plus (Nova BioMedical, Waltham, WA). IgG titer was determined by biolayer interferometry using Octet QK384 equipped with Protein A biosensors (ForteBio, Menlo Park, CA) according to the manufacturer's instructions.

Duplicates of different fed-batch cultures for the 1,030 and 4,384 cell lines were carried out in two different basal media A and B with the corresponding feed media FA and FB.

In the A + FA8 culture (basal media A, feed FA, seeding density at 8×10^5 viable cells/mL), the 1,030 or 4,384 cells were initially seeded at 8×10^5 viable cells/mL in basal media A. Feed FA (3.3% of the initial culture volume) was added to the culture once a day from day 2 onwards. Glucose was adjusted to 8 g/L on days 5 and 7, 10 g/L on days 9 and 11. Cell culture was sampled on days 2, 5, 7, 9, 11, and 13 for measuring cell growth, metabolism, and IgG expression. Additional sampling for nucleotide sugar measurement was performed on days 2, 5, 9, and 11 and for Western blot analysis on days 2 and 11. Samples for amino acid analysis were taken from the 4,384 cell culture on days 5, 7, 11, and 13. The culture was harvested on day 13 according to viability criteria.

Only the 1,030 cells were tested in the A + FA4 cultivation condition. The A + FA4 culture use same basal media and feed as the A + FA8 culture, but with a different seeding density of 4×10^5 viable cells/mL. The feeding strategy is also same as the A + FA8 process. However, no glucose addition was required in the process. Cell culture was sampled on days 2, 5, 7, 9, and 12 for cell growth, metabolism and IgG expression measurement and was harvested on day 12 according to viability criteria.

The B + FB4 culture (basal media B, feed FB, seeding density at 4×10^5 viable cells/mL) started with an initial culture (cells in basal media B with 13% initial culture volume of feed FB) at a seeding density of 4×10^5 viable cells/mL. Feed FB (10% of the initial culture volume) was added to the culture on days 2, 5, 7, 9, and 11. For the 1,030 cell line, glucose was adjusted to 6 g/L on day 5 and 9 g/L on days 9 and 11. For the 4,384 cell line, glucose was added as described above for the 1,030 cell line, although it was adjusted to 10 g/L on day 9. Cell culture was sampled on days 2, 5, 7, 9, 11, 13, and 14 for measuring cell growth, metabolism, and IgG expression. Additional sampling for intracellular nucleotide sugar quantification was carried out on days 2, 5, 9, and 11 and for Western blot analysis on days 2 and 11. For the 4,384 cell line, cell culture was also sampled for amino acid analysis on days 5, 7, 11, and 13. Fed-batch culture was harvested on day 14.

Free Amino Acid Analysis

Samples from cell culture were clarified by centrifugation at 4,500 rpm for 3 min. To precipitate and remove remaining proteins, 30 μL 4% sulphosalic acid (Sigma–Aldrich, St. Louis, MO) were added into 30 μL clarified sample of the supernatant. After centrifugation (12,000*g*, 5 min), 20 μL of the resulting suspension was collected and dried using a SpeedVac (Thermo Scientific, Waltham, MA). The dried samples were resuspended in 160 μL of start buffer, containing 0.2 M Trisodium citrate dihydrate (Sigma–Aldrich) and 0.65% v/v HNO_3 (Sigma–Aldrich) with pH = 3.1 prior to injection into the amino acid analyzer system. The system controlled by Millennium32 software (Waters, Milford, MA) is composed of two M510 pumps (Waters), two regent manager pump (Waters), a M717 refrigerated autosampler (Waters), a M474 fluorescence detector (Ex = 338 nm, Em = 455 nm) (Waters), a column oven (Waters), and a MCI-Gel CK10U column (Mitsubishi Chemical industries, Japan). All chemicals used to prepare the relevant solvents and reagents are purchased from Sigma–Aldrich. Amino acid analysis was performed using cation-exchange chromatography followed by postcolumn derivatization and fluorescence detection. Eluents used were solvent A (0.2 M Trisodium citrate dihydrate, 0.05% v/v phenol, and 5% v/v isopropanol, pH adjusted to 3.1 with nitric acid) and solvent B (0.21 M sodium borate, 5% v/v isopropanol, pH adjusted to 10.2 with NaOH). Eluents were prepared freshly and filtered by 0.2 μm filter units (Nalgene, Thermo Scientific). Chromatography was carried out using a flow rate at 0.32 mL/min and a column temperature at 62°C with the following gradient: $T_{0\,\mathrm{min}} = 0\%$ B, $T_{150\,\mathrm{min}} = 10\%$ B, $T_{28\,\mathrm{min}} = 40\%$ B, $T_{36\,\mathrm{min}} = 50\%$ B, $T_{40\,\mathrm{min}} = 100\%$ B, $T_{52\,\mathrm{min}} = 100\%$ B, $T_{53\,\mathrm{min}} = 0\%$ B. Post column oxidation and derivatization sequentially took place at 62°C in a 50 cm 0.22 mm i.d. coil with flow of hypoclorite reagent (flow rate = 0.3 mL/min) and a 150 cm 0.5 mm coil with a flow of OPA reagents (flow rate = 0.3 mL/min). Hypochlorite and OPA reagents can be prepared as described in (Barkholt and Jensen, 1989). Peak assignment and integration was done automatically with a user-defined data processing method.

Specific Metabolic Rate

The concentration of a certain nutrient or metabolite in the cell culture before feeding ($C_{x\ \mathrm{before}}$) was measured as

described above. Moreover, the concentration after feeding ($C_{x\ after}$) was calculated based on the culture volume and known addition of the proprietary feed at that time point. Additionally, the specific consumption or production rate of certain nutrient or metabolite (q_x) from time point t_1 to time point t_2 was calculated from the following equation:

$$q_x = \frac{C_{x\ before}^{t_2} - C_{x\ after}^{t_1}}{IVC^{t_2} - IVC^{t_1}},$$

in which IVC is the integral of viable cell density.

Nucleotide Sugar Analysis

Cell pellets from 2 mL cell culture samples were collected and washed with 2 mL ice-cold 0.9% w/v aqueous NaCl (Sigma–Aldrich) by centrifugation (0°C, 1,000*g*, 1 min). They were flash-frozen in liquid nitrogen and stored at −80°C until acetonitrile extraction. Under acetonitrile extraction, they were then resuspended and incubated in ice-cold 50% v/v aqueous acetonitrile (Sigma–Aldrich) on ice for 10 min prior to centrifugation (0°C, 18,000*g*, 5 min). Collected supernatant was dried in a SpeedVac (Savant, Thermo Scientific), resuspended in 240 μL water and store at −80°C until applying on HPLC for high-performance anion-exchange (HPAEC) analysis as describe in (Jimenez Del Val et al., 2013).

IgG Purification

Harvested cell culture was centrifuged at 4,500*g* for 20 min using Multifuge 3SR (Hereaus, Thermo Scientific). The supernatant was filtered through a 0.22 μm filter (Millipore, Billerica, MA) prior to application onto the self-packed MabSelect SuRe ProteinA column, which contains 200 μL of MabSelect SuRe protein A resin slurry (GE Healthcare, Fairfield, CA) equilibrated with PBS. IgG was captured by the column and eluted by 500 μL of 0.1 M citrate with pH 3.5. The elution was immediately subjected to a buffer exchange procedure by passing through a NAP-5 column (GE Healthcare) equilibrated by a formulation buffer containing 10 mM Citrate (Sigma–Aldrich) and 150 mM NaCl (Sigma–Aldrich) with pH 6.0. IgG concentration was measured using NanoDrop ND-1000 (Thermo Scientific). Purified IgG was stored at −20°C until further analysis.

Intact Mass Analysis of IgG

Intact mass analysis of the purified IgG was performed on a LC–MS system using Dionex Ultimate 3000 RSLC System equipped with Ultimate 3000 RS variable wavelength detector (Dionex, Sunnyvale, CA) and Mass Prep micro desalting 2.1 × 5 mm column (Waters) in conjunction with micrOTOF-Q II (Bruker, Billerica, MA). The flow rate was 0.2 mL/min. The gradient with solvent A (water with 0.1% formic acid; Sigma–Aldrich) and solvent B (acetonitrile with 0.1% formic acid; Sigma–Aldrich) was as follow: $T_{0\,min}$ = 5% B, $T_{2\,min}$ = 5% B, $T_{2.1\,min}$ = 90% B $T_{5\,min}$ = 90% B, $T_{5.1\,min}$ = 30% B, $T_{6\,min}$ = 30% B, $T_{7\,min}$ = 90% B, $T_{7.1\,min}$ = 5%, $T_{11\,min}$ = 5%. The UV detection was performed at 215 nm. The different combinations of glycans on the IgG was analyzed and quantified according to the peak intensity of each isoform in the intact mass spectrum of IgG using Bruker Compass Data Analysis 4.2 software (Bruker).

Glycoprofiling of IgG

IgG glycoprofiling was carried out using GlykoPrep® InstantAB™ kit (Prozyme, Hayward, CA) for quantifying the total of each *N*-glycans. Digestion, labeling and cleanup of *N*-glycans from IgG was performed according to the manufacturer's instructions. Labeled glycans were buffered in 50% v/v aqueous acetonitrile prior to the HPLC analysis using Dionex Ultimate 3000 RSLC System equipped with Ultimate 3000 RS fluorescence detector (Dionex) and ACQUITY UPLC BEH Glycan 1.7 μm, 2.1 × 150 mm column (Waters). The mobile phase used was solvent A (100% acetonitrile; Sigma–Aldrich) and solvent B (100 mM ammonium formate with pH = 4.5; BDH-Merck, Poole, UK). Elution of the sample was performed using the following flow rate and gradient: $T_{0\,min}$ = 25% B with flow rate = 0.5 min/mL, $T_{5\,min}$ = 25% B with flow rate = 0.5 min/mL, $T_{51.5\,min}$ = 40% B with flow rate = 0.5 min/mL, $T_{53\,min}$ = 100% B with flow rate = 0.25 min/mL, $T_{58\,min}$ = 100% B with flow rate = 0.25 min/mL, $T_{60\,min}$ = 25% B with flow rate = 0.5 min/mL, $T_{70\,min}$ = 25% B with flow rate = 0.5 min/mL, $T_{75\,min}$ = 25% B with flow rate = 0.5 min/mL. Fluorescence detection were performed at Ex = 278 nm and Em = 344 nm. Analysis of the chromatogram was performed with Chromeleon software (Dionex). Relative quantification was performed using peak area and peak assignment based on retention time of known standards.

Western Blot Analysis

Cell pellets from culture samples were washed with PBS (Invitrogen, Life Technologies, Carlsbad, CA) and lysed in RIPA buffer (Thermo scientific) in the presence of protease inhibitor cocktail (Thermo scientific) on ice. The lysates were sonicated and centrifuged for 2 min at 14,000 G. Total protein concentration in the collected supernatant was quantified by pierce BCA protein assay kit (Thermo scientific). NuPAGE sample loading buffer and reducing buffer (Invitrogen, Life Technologies) were added as required for each supernatant sample containing same amount of total protein. Samples were heated at 90°C for 10 min prior to loading onto NuPAGE 4–12% Bis–Tris gel (Invitrogen, Life Technologies). Electrophoresis was run at 150 V for 1 h using MES buffer (Invitrogen, Life Technologies). Proteins were transferred to nitrocellulose membrane using iBlot system (Invitrogen, Life Technologies). Membrane was blocked in Odyssey blocking buffer (LI-COR) for 1 h (room temperature, 50 rpm), probed with goat anti-MGAT1 antibody (1:1,000; Abcam, Cambridge, UK) and rabbit anti-SLC35A3 antibody (1:1,000; Abcam) and rabbit anti β-actin antibody (1:1,000; Cell Signaling, Danvers, MA) over night (4°C, 50 rpm) and

washed with TBS (BioRad, Hercules, CA) with 0.1% Tween 20 (Millipore, Billerica, MA). After 1 h incubation (room temperature, 50 rpm) with IR Dye 800 CW-conjugated donkey anti-goat and anti-rabbit antibody (1:5,000; LI-COR, Lincoln, NE), the membrane was washed again and subjected to fluorescence detection at 800 nm using Odyssey Scanner (LI-COR). Bands in Western blot were analyzed using image studio lite software (LI-COR).

Results

The B + FB4 culture (basal media B, feed FB, seeding density at 4×10^5 viable cells/mL) is the proprietary first-generation upstream process developed by Symphogen with optimal process parameter fitting with media B and feed FB for most of the IgG-producing cell lines generated by Symphogen. During in-house upstream optimization, we found media A with feed FA has potentially better media capacity for cell growth and antibody production in some cell lines if the cell culture starts at a suitable seeding density (data not shown). Here, we test the A + FA4 (basal media A, feed FA, seeding density at 4×10^5 viable cells/mL), A + FA8 (basal media A, feed FA, seeding density at 8×10^5 viable cells/mL) and B + FB4 cultures in order to demonstrate how the nutrients (glucose and amino acids) were used differently during the fed-batch culture and what the IgG titer and glycosylation quality were in relation to that.

Culture Behavior and IgG Production

Culture behavior and IgG production constitute essential information for assessing media, feeds and overall upstream process performance. Figure 1 shows the effect of different upstream processes on growth, metabolism and IgG production for two model cell lines 1,030 and 4,384. In general, the durations of A + FA4 and A + FA8 cultures were slightly shorter than the B + FB4 culture. Notably, the A + FA8 culture resulted in faster cell growth and increased the integral of viable cells (IVC) for either cell line compared to the B + FB4 culture. More specifically, in Figure 1A, when using the B + FB4 cultivation condition for the 1,030 and 4,384 cell lines, the peak viable cell concentrations were about 5 and 15×10^6 cells/mL on day 11, respectively. In contrast, the peak viable cell densities were about 15 and 20×10^6 cells/mL already on day 9 in the A + FA8 culture for the 1,030 and 4,384 cell line, respectively. Interestingly, the A + FA4 culture did not exhibit any significant improvement on cell growth compared to the B + FB4 culture. Decline in viability

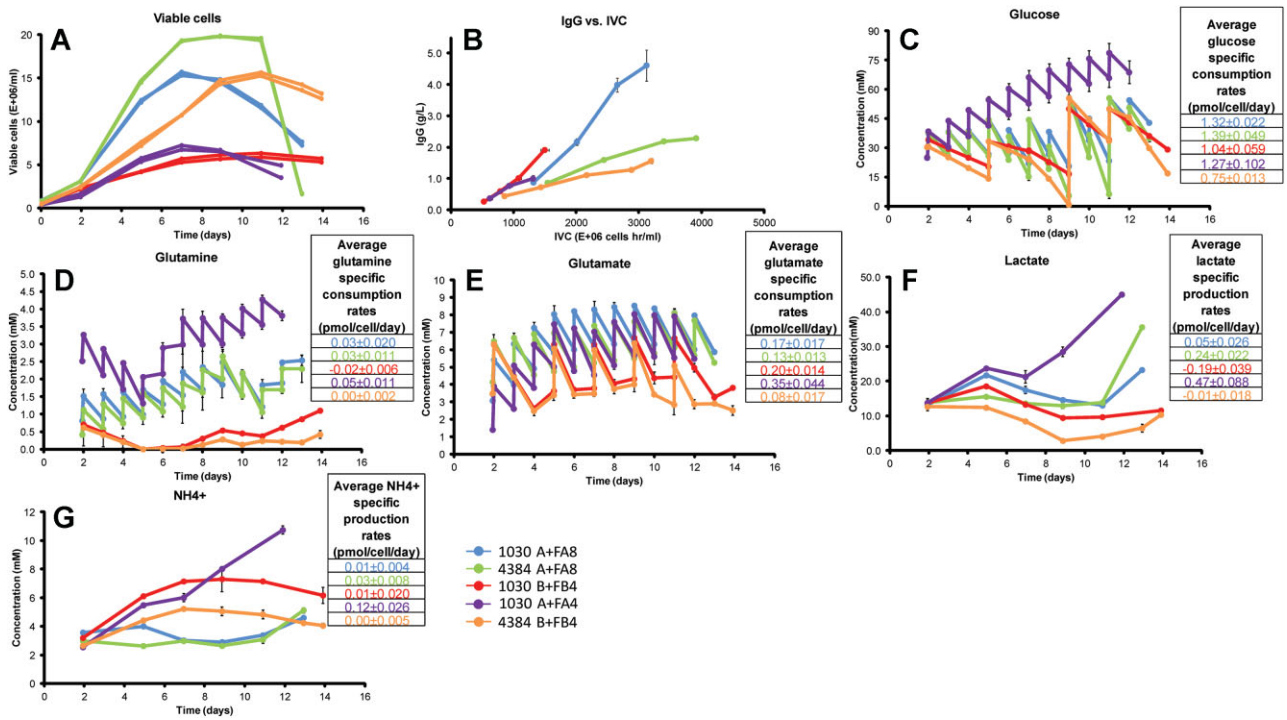

Figure 1. Comparison of five fed-batch cultures with different cell lines and cultivation conditions. Viable cell density and integral of viable cells (IVC) versus IgG titer are presented in (**A**) and (**B**), respectively. Time courses of Glucose (**C**), Glutamine (**D**), Glutamate (**E**), Lactate (**F**), and Ammonia (**G**) concentrations are also shown. The error bars correspond to one standard deviation calculated from duplicate experiments. In (C), (D), and (E) the data points from B + BA4 culture and A + FA8 culture on days 3, 4, 6, 8, 10, and 12 and from A + FA4 culture on days 3, 4, 6, 8, 10, 11 are unmeasured pseudo points calculated by assuming the consumption rate is constant between the measured points. Average of specific consumption/production rate of certain metabolite was also calculated based on specific consumption/production rate of certain metabolite on each measured time point from day 7 to the harvest (same color codes are used for indicating the cultivation conditions).

occurred earlier and faster in the A + FA4 and A + FA8 cultures than in the B + FB4 culture (Fig. S1A). For either the 1,030 or 4,384 cell line, the A + FA8 culture lead to considerably higher IgG production than the other cultures, as a result of both high cell growth and high specific productivity of IgG (Fig. 1B).

Although the different cultivation conditions are observed to influence specific IgG productivity (q_p), the average q_p of each cell line is relatively constant and calculated to be 40.7 pg/cell/day for 1,030 and 14.2 pg/cell/day for 4,384, as seen in Figure S3.

As a consequence of consumption and feeding, glucose concentration fluctuated at slightly higher level in the A + FA8 culture compared to the B + FB4 culture. Also, quite noticeably, glucose largely accumulated during the A + FA4 culture (Fig. 1C). The accumulation of glutamine after the temperature shift in the A + FA4 culture reached 3.5 mM at harvest. Additionally, the concentration of glutamine was around 1–2 mM before feeding in the A + FA8 culture for both cell lines compared to around 0–1 mM in the B + FB4 culture (Fig. 1C). Glutamate was generally maintained at a higher concentration before feeding in the A + FA8 culture (around 3–6 mM) than in the B + FB4 culture (around 2–4 mM) throughout the fed-batch process (Fig. 1E). The average specific glucose and glutamine consumption rates from day 7 to harvest were found to be generally higher in the A + FA8 culture than in the B + FB4 culture for both cell lines (Fig. 1D and E).

In terms of by-product formation, the accumulation of lactate in the A + FA8 culture was higher than that in the B + FB4 culture for both cell lines (Fig. 1F). In the A + FA4 culture, both lactate accumulation and its average specific production rate were particularly high, which may due to the high glucose concentration in this culture (Fig. 1F). Accumulation of $NH4^+$ in the A + FA8 culture was lower than that in the B + FB4 culture for both cell lines from day 5 to 11 (Fig. 1G). However, in the A + FA4 culture, the accumulation of $NH4^+$ increased dramatically from 2 up to 10 mM during the culture, which also demonstrated a particularly high average $NH4^+$ specific production rate (Fig. 1G).

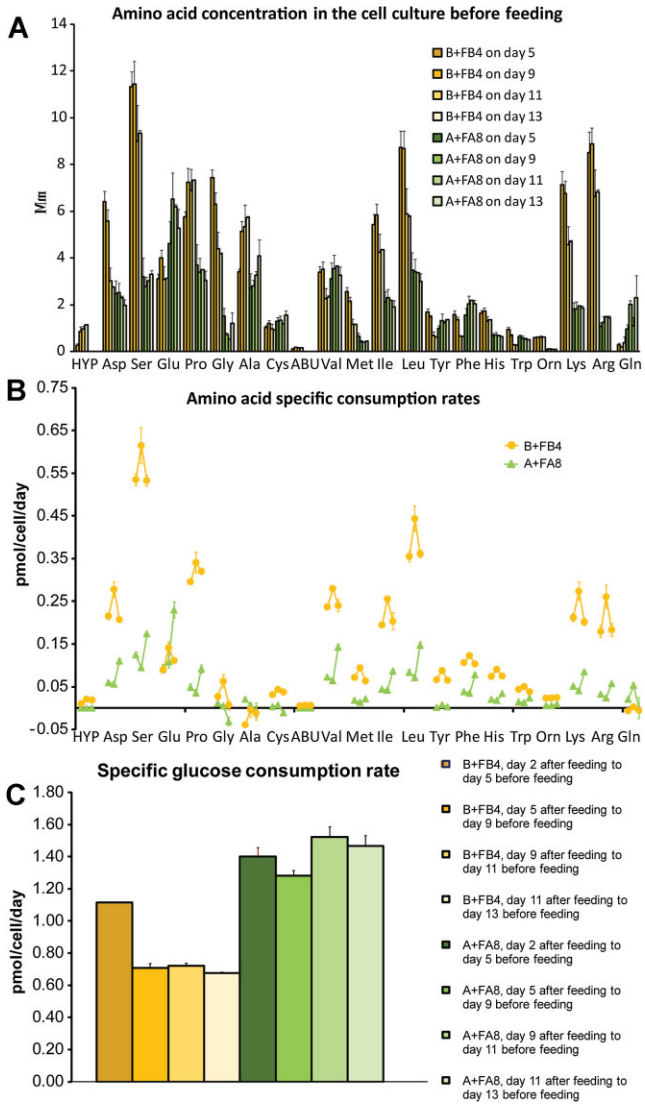

Figure 2. Glucose and amino acids metabolisms of 4,384 cell line in A + FA8 and B + FB4 cultures. (**A**) Amino acid concentrations on day 5, 9, 11, 13 in the cell culture before feeding. All amino acids were measured by free amino acid analysis, except glutamine, which was measured by Bioprofile 100 plus. Glutamine, threonine, and asparagine eluted as one peak and their concentration cannot be resolved in the chromatogram of the free amino acid analysis. (**B**) Specific consumption rates of amino acids: from day 5 after feeding to day 9 before feeding (left point), from day 9 after feeding to day 11 before feeding (middle point), from day 11 after feeding to day 13 before feeding (right point). (**C**) Specific consumption rate of glucose.

Amino Acid and Glucose Metabolism

To further understand the culture differences among the cultivation conditions and cell lines tested, the concentrations and specific consumption rates of amino acids and glucose have been assessed. In general, amino acid concentrations for 4,384 cells were more stable in the A + FA8 culture than in the B + FB4 culture between day 5 and 13 (Fig. 2A). Specifically, amino acids such as Asp, Ser, Gly, Val, Met, Ile, Leu, Lys, Arg, and all the aromatic amino acids (Tyr, Phe, His, and Trp) have a clear decline from day 11 onwards in the B + FB4 culture. However, Ala accumulated in both A + FA8 and B + FB4 cultures from day 5 to 13. The majority of amino acids have higher concentration on days 5, 9, 11, and 13 in the B + FB4 culture, apart from Glu and Gln on days 5, 9, 11, and 13 and Cys, Val, and aromatic amino acids (Tyr, Phe, Trp) on days 11 and 13. Interestingly, the specific amino acid consumption rates are very much dependent on the concentration of corresponding amino acids in the culture. It was indicated by the fact that the specific amino acid consumption rates (except Glu, Gln, and Ala) were higher from day 5 to 13 in the B + FB4 culture. Conversely, the specific glucose consumption rate was always higher in the A + FA8 culture from day 5 to 13 (Fig. 2B and C). We also found that the specific consumption rates of amino acids in the B + FB4 culture in early stationary phase (day 9–11) were higher than in growth phase (day 5–9) and late stationary phase (day 11–13). Conversely, the specific consumption rates

of amino acids (except Glu, Gln, Ala, Cys, Tyr, HYP, and ABU) in the A + FA8 culture are lower in early stationary phase (day 9–11) than in growth phase (day 5–9) and late stationary phase (day 11–13). Furthermore, the specific glucose consumption during the cell culture declined after the temperature shift (day 5) in the B + FB4 culture but was stable in the A + FA8 culture.

Nucleotide Sugar Metabolism

Nucleotide sugars are the donors of sugar chain elongation reactions in glycosylation; they are therefore thought to be one of the major factors that affect the final glycopatterns of the IgG. As shown in Figure 3, nucleotide sugars measured in this study were synthesized from glucose through two pathways: the UDP-Glc/UDP-Gal/UDP-GlcA pathway and the UDP-GalNac/UDP-GlcNac pathway. In general, there was considerable accumulation of UDP-GlcNAc and UDP-GalNAc during the culture. In addition, their concentration was cell line-dependent (higher in 1,030 cell line than in 4,384 cell line under both cultivation conditions), and both species in 1,030 cell lines were more sensitive to cultivation condition changes.

Interestingly, the accumulation of UDP-GalNAc, UDP-GlcNAc and UDP-GlcA has a rather similar trend. Conversely, UDP-Gal and UDP-Glc accumulate to rather lower concentrations compared to UDP-GlcNAc and UDP-GalNAc, exhibiting similar profiles. Furthermore, their concentration was both cell line-dependent (higher in 1,030 cell line than in 4,384 cell line in either cultivation condition) and cultivation condition-dependent (higher in A + FA8 culture than B + FB4 culture for either cell line).

Abbreviated Reaction Network of Glycosylation Pathway

An abbreviated reaction network is shown in Figure 4 illustrating the sequence of reactions that occur to produce the IgG-bound glycans that were identified in this work.

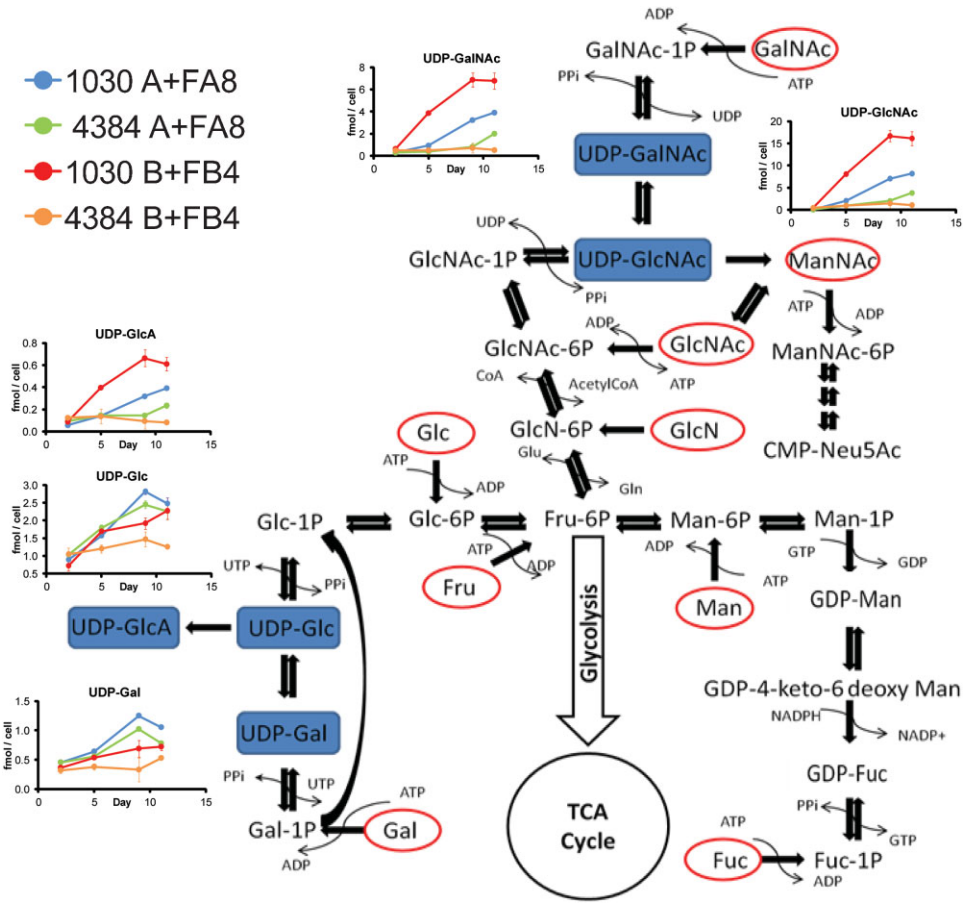

Figure 3. Intracellular nucleotide sugar analysis of cell lysates from fed-batch. Nucleotide sugar synthesis typically starts from degradation of glucose through glycolysis, in which glucose converts into glucose-6-phosphate and fructose-6 phosphate. Glucose-6-phosphate becomes UDP-glucose (UDP-Glc), UDP-galactose (UDP-Gal), and UDP-glucuronic acid (UDP-GlcA) through a series of enzymatic reactions. On the other hand, fructose-6 phosphate supplying further glycolysis and TCA cycle for energy gain can also be directed into two major nucleotide sugar synthesis pathways. One can generate UDP-glucosamine (UDP-GlcNAc) and UDP-galactosamine (UDP-GalNAc). The other one can produce GDP-mannose (GDP-Man) and GDP-fucose (GDP-Fuc). Galactose, mannose, fructose as well as other sugars illustrated in the figure with red circle can also be used as substrates for nucleotide sugar synthesis other than glucose. Nucleotide sugars measured in this study were shown in blue box.

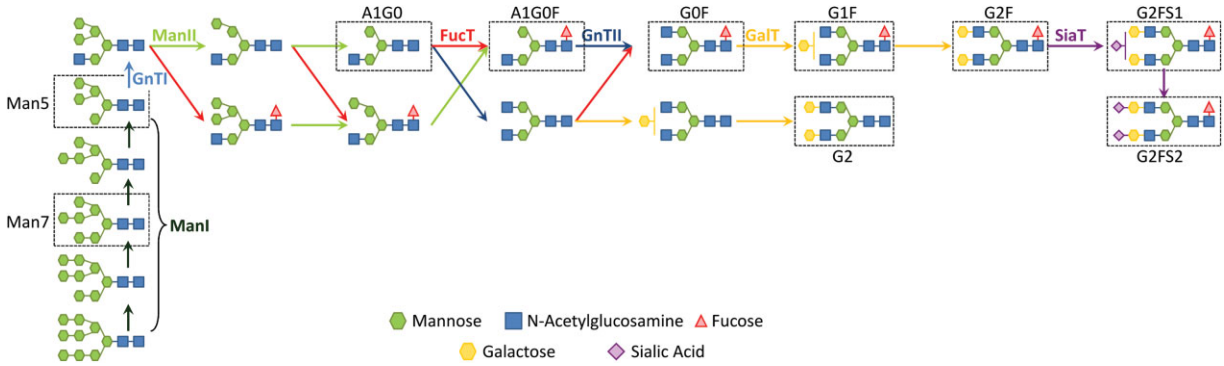

Figure 4. Simplified reaction scheme for IgG Fc *N*-glycosylation. The network begins with a nine mannose oligosaccharide structure, which is sequentially cleaved by α-mannosidase I (ManI) until a five mannose structure is produced (Man5). An *N*-acetylglucosamine residue (GlcNAc) is then added to the Man5 glycan by action of the α-1,3-mannosyl-glycoprotein 2-β-*N*-acetylglucosaminyltransferase (GnTI). After this point, the reaction scheme diverges into two branches, depending on the order in which the reactions occur. Regardless of the order, after the GnTI-catalyzed reaction, additional mannose residues are removed by α-mannosidase II (ManII) to yield the A1G0 glycan. Subsequently, a fucose residue is added by the 6-α-fucosyltransferase enzyme (FucT) to produce A1G0F, followed by addition of a second GlcNAc residue by α-1,6-mannosyl-glycoprotein 2-β-*N*-acetylglucosaminyltransferase (GnTII) to generate the G0F glycan. The reaction sequence concludes with addition of galactose and sialic acid residues to each arm of the biantennary glycan by means of β-1,4 galactosyltransferase (β-GalT) and α-2,6/α-2,3 sialyltransferase (SiaT), respectively. Addition of these monosaccharides produces the G1F, G2, G2F, and G2FS1 glycans.

Glycosylation of IgG

Intact mass analysis was carried out mainly to provide relative quantification of glycan combinations at the *N*-glycosylation sites of the IgG. Table I shows the glycan combinations on the IgG and their molecular weights that can typically be resolved from the mass spectrum. As shown in Figure 5, the A + FA8 and A + FA4 cultures led to a lower amount of relatively immature glycoform combinations (Man5/Man5, Man5/A1G0F, and A1G0F/G0F) but higher amounts of relatively mature glycoform combinations (G0F/G1F, G1F/G1F or G0F/G2F, and G1F/G2F) than the B + FB4 culture. Particularly, the Man5/Man5 combination from the A + FA8 culture was less than the detectable level of the analytical method used. We also noticed that the 4,384 cell line produced more relatively immature glycoform combinations than the 1,030 cell line in both A + FA8 and B + FB4 cultures. The results were confirmed by glycoprofiling using instant AB labeling, an analysis providing higher resolution (Fig. 6). As shown in Figure 6A and B, the distribution for all cultures ranges from immature glycan structures such as Man7 to highly processed structures such as the G2FS1. The most abundant glycans were found to be G0F, G1F, Man5, and A1G0F. More Man5, G1F, G2F, and G2FS1 were produced by 4,384 cell line than

Table I. Typical glycan combinations on the IgG resolved from intact mass.

Glycan combinations on the IgG	Detected intact mass of IgG (Da)
NG/NG	$MW_{IgG\text{-}NG/NG}$[a]
G0F/NG	$MW_{IgG\text{-}NG/NG} + 1{,}445$[a]
Man5/Man5	$MW_{IgG\text{-}NG/NG} + 2{,}434$
Man5/A1G0F	$MW_{IgG\text{-}NG/NG} + 2{,}458$
A1G0F/A1G0F	$MW_{IgG\text{-}NG/NG} + 2{,}482$
A1G0F/G0F	$MW_{IgG\text{-}NG/NG} + 2{,}687$
G0F/G0F	$MW_{IgG\text{-}NG/NG} + 2{,}891$
G0F/G1F	$MW_{IgG\text{-}NG/NG} + 3{,}053$
G1F/G1F or G0F/G2F	$MW_{IgG\text{-}NG/NG} + 3{,}215$
G1F/G2F	$MW_{IgG\text{-}NG/NG} + 3{,}377$
G2F/G2F	$MW_{IgG\text{-}NG/NG} + 3{,}539$

$MW_{IgG\text{-}NG/NG}$ is the molecular weight of the non-glycosylated (NG) IgG in question.

[a]Detectable only in high abundance.

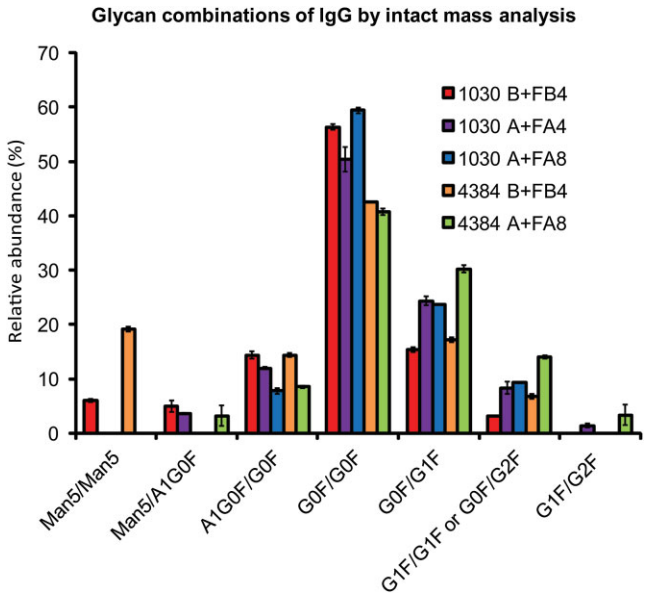

Figure 5. Relative abundance of glycan combinations of IgG detected by intact mass analysis.

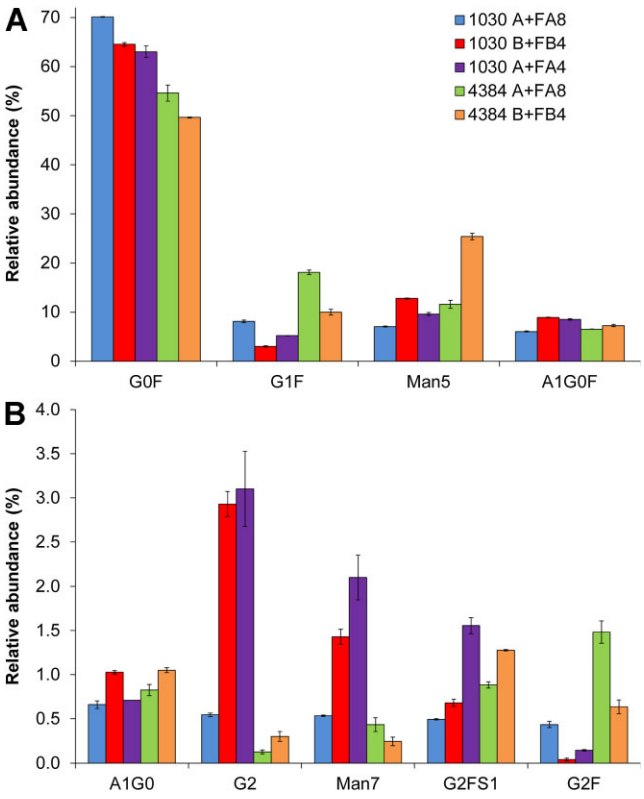

Figure 6. Analysis of IgG glycosylation by Instant-AB labeled glycoprofiling. (**A**) and (**B**) Glycan distribution as determined by HPLC.

1,030 cell line in the same cultivation condition. However, cell line 1,030 produces more Man7 than cell line 4,384, regardless of the cultivation condition. Furthermore, the A + FA8 culture gives rise to less Man5 and A1G0F, but more G1F and G2F than the B + FB4 culture.

Western Blot Analysis of GnT1 and UDP-GlcNAc Transporter

Cell pellets (1,030 and 4,384) from day 2 and 11 of the A + FA8 and B + FB4 cultures were collected for Western blot analysis (Fig. S2). The expression levels of GnT1 and UDP-GlcNAc transporter were analyzed with the purpose of understanding the very first steps of the glycan chain elongation reaction in the Golgi, in which UDP-GlcNAc is transported into the organelle and then added onto the Man5 glycan structure. All measurements were first normalized to the internal standard β-Actin and further normalized to the condition of the 1,030 cell line in the A + FA8 culture on day 2. In Figure 6, the expression of GnTI at both time points seems to be cultivation condition-independent for 1,030 cells. However, a clear difference can be observed for UDP-GlcNAc transporter expression in 1,030 cells. Culture 1,030 A + FA8 shows basal levels of UDP-GlcNAc transporter expression on day 2, which then decrease by ~50% by day 11. In contrast, culture 1,030 B + FB4 shows slightly low level at day 2, which increases dramatically (~2-fold) by day 11. Expression profiles for both GnT1 and UDP-GlcNAc transporter were similar for the 4,384 cell line, regardless of cultivation conditions. We also noticed that the level of GnT1 was lower in the B + FB4 culture at both time points than in the A + FA8 culture.

Discussion

The understanding of how different nutrients were consumed for different cell activities, specifically cell growth, metabolism and protein production, provides crucial insight for media and process optimization. Our data indicate that faster cell growth, higher IVC and IgG production, and more mature glycopatterns can be obtained as the result of more balanced amino acid concentration in the culture and higher glucose consumption rate when we transition from the B + FB4 to the A + FA8 culture for both 1,030 and 4,384 cell lines. A number of important factors that correlated with the cell growth, specific productivity and glycosylation have been identified in this study.

Oxidative Metabolism and By-Product Formation in Correlation With Cell Growth

In the A + FA8 culture, higher glucose consumption compared to the B + FB4 culture implies that glucose is the major source for energy gain, despite leading to higher lactate levels. It is probably also the main reason why cells in A + FA4 media grow faster and to higher cell density. We have also noticed that more lactate was consumed from day 5 to 11 in the B + FB4 culture. This observation agrees with previous CHO metabolic flux studies that report that exponential growth phase is characterized by lactate production and high glycolysis rate and TCA flux, whereas in stationary phase cells demonstrate lactate consumption, lower glycolysis rate and TCA flux (Ahn and Antoniewicz, 2011; Carinhas et al., 2013). In contrast, we found higher specific glucose consumption rates and higher lactate, Gly and Ala specific production rates in stationary phase (day 9–11) than in late growth phase (day 5–9) of the A + FA8 culture. In fact, leaking from glycolysis is thought to balance the cytosolic NAD/NADH level, so the capacity of the TCA cycle is not exceeded (Mulukutla et al., 2012). When comparing B + FB4 with A + FA8 culture, positive Ala specific production rate, higher Ile and Leu specific consumption rates and higher specific consumption rates of Glu and its possible supplier Pro, His, and Arg indicate higher transamination activities of cells (Chen and Harcum, 2005; Schmelzer and Miller, 2002) and thus more intermediates for entering the TCA cycle in B + FB4 culture. Faster accumulation of $NH4^+$ in the growth phase of the B + FB4 culture also provides evidence for oxidative metabolism by means of converting Gly, Ser, and Cys to pyruvate and glutamate to α-ketoglutarate. The high accumulation of $NH4^+$, which is thought to inhibit cell growth (Altamirano et al., 2013), could also be one of the important downsides of

the B + FB4 culture in contrast to the A + FA8 culture. In the A + FA4 culture as an extreme case, very high lactate and $NH4^+$ concentrations inhibited cell growth as a consequence of unbalanced nutrient supply to cell activities. Interestingly, Leu has previously been reported to have a detrimental effect on cell growth (Gonzalez-Leal et al., 2011). Therefore, reducing its concentration as in the A + FA8 process appears to be beneficial. It is also worth mentioning that the different behaviors with respect to specific glucose consumption rate from day 5 onwards in the A + FA8 and B + FB4 cultures might not be a direct response to temperature shift and change in growth rate. This would be consistent with previous results showing that the specific glucose consumption is not affected by either temperature reduction or low specific growth rate (Vergara et al., 2014). A possible explanation for such a difference might be that the requirement of glucose and the redistribution of carbon flux for biomass and lactate accumulation in different growth phases depended on the nutrient concentrations in the culture.

Amino Acid Metabolism in Correlation With Specific Productivity

Ser and Leu were the two amino acids with the highest consumption rates in the B + FB4 culture. The fast consumption of Ser and Leu can be attributed to their abundance in the amino acid composition of the produced 4,384 antibody (Table SI). It is also reasonable to find that Arg, which has been reported to have a negative effect on mAb production in CHO DG44 cell culture (Gonzalez-Leal et al., 2011), is present at lower concentrations in A + FA8 culture than B + FB4 culture. More amino acids consumed entered the catabolic process in B + FB4 culture than in A + FA8 culture, in order to complement the energy gain from glucose. Therefore, the building blocks for IgG production may be less and the specific productivity in B + FB4 culture may thus be negatively affected.

Factors that Affect Glycosylation

Here, we also present the mAb Fc *N*-glycosylation distributions resulting from different cell lines cultured in two media with appropriately formulated feeding strategies. In order to identify the cause for the observed differences in glycan profiles, the mechanisms that determine the glycosylation process must be considered.

Product-Associated Mechanisms

The first property that controls *N*-glycosylation is the accessibility of the protein-bound glycan for action by glycosidases and glycosyltransferases. For example, the limited presence of galactose and sialic acid on the Fc glycans of mAbs has, in some cases, been attributed to these effects (Hills et al., 2001; Wormald et al., 1997). This limitation depends solely on the tertiary and quaternary structure of the recombinant protein, and is independent of metabolic and protein expression effects.

Resident Protein-Associated Mechanisms

The second mechanism that influences glycan processing is the abundance and activity of glycosylation-associated Golgi resident proteins relative to the specific productivity of the recombinant protein. The Golgi resident proteins most closely involved in protein glycosylation are nucleotide sugar transport proteins and glycosylation enzymes (glycosidases and glycosyltransferases). Gene expression of these Golgi resident proteins has been reported to vary during cell culture (Pacis et al., 2011; Wong et al., 2010a) and overexpression of glycosyltransferases (Umana et al., 1999; Weikert et al., 1999) and NS transport proteins (Wong et al., 2006) has been used to control or remodel the glycosylation patterns of therapeutic proteins produced in CHO cells. Additional reports have suggested that activity and localization of Golgi resident proteins may be influenced by certain process conditions, such as ammonia accumulation and concomitant changes in culture pH. Specifically, elevated culture pH has been associated with reduced galactosyltransferase and sialyltransferase activities (Gawlitzek et al., 2000; Muthing et al., 2003; Yoon et al., 2005) and mislocalization of glycosyltransferase enzymes within the Golgi apparatus (Rivinoja et al., 2009). In addition, pH has also been reported to impact UDP-GlcNAc transport into the Golgi apparatus by modifying the ionisation state of UMP, which is the anti-port substrate used by the UDP-GlcNAc transport protein (Waldman and Rudnick, 1990).

Metabolic Mechanisms

The third mechanism that determines glycan processing is the availability of nucleotide sugars within the Golgi apparatus lumen. Addition of monosaccharides to the protein-bound glycans requires nucleotide sugars as co-substrates. When these species are in low abundance in the Golgi lumen, the extent of glycosylation reactions decreases. Reduced nucleotide sugar concentration within the Golgi apparatus may result from limited transport of these species into the Golgi apparatus (Weikert et al., 1999; Wong et al., 2006) or from nutrient limitations during their biosynthesis (Kochanowski et al., 2008). Specifically, availability of UDP-GlcNAc has been reported to be closely linked with glutamine availability during cell culture (Chee Furng Wong et al., 2005; Nyberg et al., 1999) and strategies to increase the availability of this NS have relied on supplementing culture media with glucosamine and uridine (Baker et al., 2001; Hills et al., 2001). Similarly, availability of UDP-Gal has been linked with glucose metabolism and efforts to control galactosylation of therapeutic proteins have relied on supplementing cell cultures with uridine, manganese, and galactose (Grainger and James, 2013; Gramer et al., 2011).

When analyzing our data for recombinant protein glycosylation within this mechanistic context, we see that the presence of certain glycans results from both resident protein availability and metabolic effects. The relative abundance of Man7 correlates with the specific productivity of each cell line.

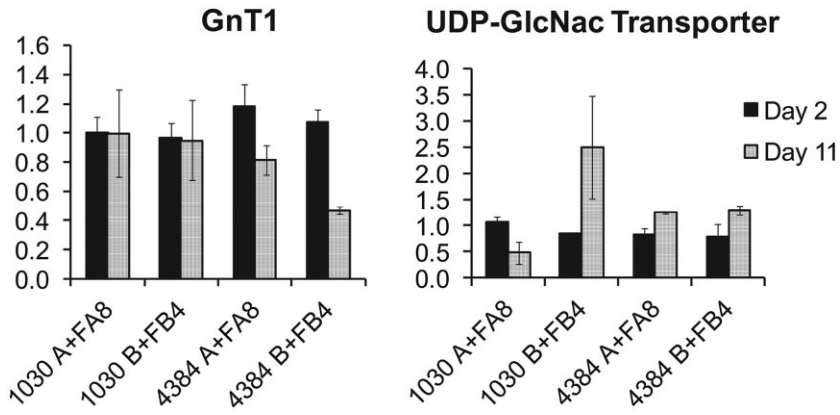

Figure 7. Quantification of intracellular GnT1 and UDP-GlcNac transporter levels by Western blot.

Cell line 1,030, which has the highest average q_p (see Fig. S3), produces more Man7 (up to 2.1% ± 0.25%) than cell line 4,384 (up to 0.43% ± 0.08%). It is possible that this occurs because the 1,030 cells have insufficient alpha mannosidase II (ManII) availability to cope with their higher q_p.

In contrast to the Man7 glycan, presence of Man5 can occur because of low abundance or activity of Golgi resident proteins (UDP-GlcNAc transporter and GnTI) or low intracellular availability of UDP-GlcNAc. Despite similar UDP-GlcNAc transporter expression levels, 4,384 cells produce 2.2-fold ± 0.2 ($P = 0.000022$) more Man5 in B + FB4 culture than in A + FA8 culture (Fig. 6). This indicates that, for this cell line, accumulation of the Man5 glycan is likely due to the bottleneck in availability of UDP-GlcNAc and expression of GnT1. This is further confirmed by Figure 3 where the 4,384 cell line was found to have extremely low intracellular UDP-GlcNAc concentration and Figure 7 where this cell line exhibited lower expression level of GnT1 on both day 2 and 11 in B + FB4 culture. We must emphasize that low intracellular nucleotide sugar concentration may occur due to low levels of biosynthesis or high levels of consumption. Given the low GlcNAc occupancy (Fig. 8A) and high amount of Man5 that accumulates for culture 4,384 B + FB4 compared to those of culture 4,384 A + FA8, it is likely that the low intracellular UDP-GlcNAc concentration for the former is due to low biosynthesis of this nucleotide sugar, whereas the low UDP-GlcNAc concentration observed for 4,384 A + FA8 is likely due to high consumption of this

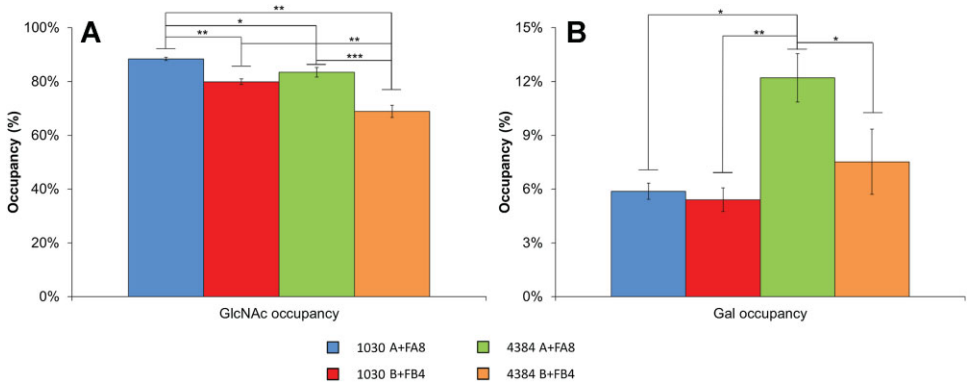

Figure 8. Intracellular NSD concentration and average monosaccharide occupancy on glycans. The percentage of GlcNAc occupancy in all measured glycans is presented in (**A**) and occupancy of galactose is presented in (**B**). GlcNAc occupancy was calculated assuming that 100% occupancy involves two moles of GlcNAc being added to all glycans in Golgi: $GlcNAc_{occ} = (2*G0F + 2*G1F + 0*Man5 + 1*A1G0F + 1*A1G0 + 2*G2 + 0*Man7 + 2*G2FS1 + 2*G2F)/2$. Similarly, galactose occupancy was calculated assuming that 100% corresponds to two moles of galactose being added to all glycans within the Golgi: $Gal_{occ} = (0*G0F + 1*G1F + 0*Man5 + 0*A1G0F + 0*A1G0 + 2*G2 + 0*Man7 + 2*G2FS1 + 2*G2F)/2$.

nucleotide sugar. Limited biosynthesis of UDP-GlcNAc in culture B + FB4 is substantiated by the low extracellular glutamine availability in this culture (Fig. 1D). Limited availability of this nutrient has been widely reported to limit UDP-GlcNAc biosynthesis (Chee Furng Wong et al., 2005; Kochanowski et al., 2008; Nyberg et al., 1999).

Cell line 1,030 exhibits rather different behaviors. In culture B + FB4, 1,030 cells produce 81.1% ± 3.5% ($P < 0.0001$) more Man5 and 8.3% ± 0.9% ($P = 0.00055$) lower overall GlcNAc occupancy than in the A + FA8 culture. This contrasts heavily with the intracellular UDP-GlcNAc concentration data (Fig. 3), where the culture that generates lowest GlcNAc occupancy and highest Man5 secretion exhibits higher UDP-GlcNAc availability. Therefore, UDP-GlcNAc concentration may not be the limiting factor for the glycosylation processing in this cell line. It is also correlated with previous findings that feeding GlcNAc, although increased intracellular concentration of UDP-GlcNAc (Wong et al., 2010b), could not decrease the level of Man5 or A1G0F of the IgG produced (unpublished data). High UDP-GlcNAc accumulation, high Man5 secretion and a lower overall GlcNAc occupancy can occur if the nucleotide sugar is being consumed at a lower rate than that at which it is being produced. Reduced consumption of UDP-GlcNAc may be attributed to insufficient expression of GnTI or UDP-GlcNAc transporter. However, Figure 7 shows that GnTI is expressed at similar levels in both cultivation conditions for cell line 1,030, suggesting that enzyme expression may not be limiting. We also see that cell line 1,030 in the B + FB4 culture presents a two-fold increase in expression of the UDP-GlcNAc transporter transporter by day 11 of culture despite having slightly lower expression of this transporter on day 2. This suggests that availability of UDP-GlcNAc transporter is also non-limiting. With this analysis, the only remaining causes for reduced UDP-GlcNAc consumption involve the activity of GnTI or UDP-GlcNAc transporter. We also found that high extracellular ammonia accumulation in this cell line correlates with low GlcNAc occupancy and high Man5 secretion. Previous reports have proposed that ammonia accumulation may increase the pH within the Golgi apparatus, thus inhibiting the activity of glycosylation enzymes (Borys et al., 1994; Gawlitzek et al., 2000). It has also been reported that increased Golgi pH causes mislocalization of glycosyltransferases (Rivinoja et al., 2009) and impacts UDP-GlcNAc transport into Golgi by modifying the ionisation state of UMP, which is the anti-port substrate used by UDP-GlcNAc transporter (Waldman and Rudnick, 1990).

Similarly to GlcNAc occupancy, the addition of galactose to mAb Fc glycans depends both on glycosyltransferase availability and intracellular nucleotide sugar concentration. In addition, however, low abundance of galactose on mAb Fc glycans has also been associated with decreased accessibility of GalT to the oligosaccharides present on this site (Hills et al., 2001; Wormald et al., 1997). Figure 8B shows that cell line 1,030 produces similar levels of galactose occupancy under both tested cultivation conditions. In contrast, culture 4,384 A + FA8 leads to 38.4% ± 16.4% ($P = 0.023$) higher galactose occupancy than culture B + FB4 with the same cell line, indicating that for 4,384 cells, galactosylated glycan production is cultivation condition-dependent. Despite this, the data shows that, on average, 4,384 cells generate higher galactosylation.

This may be attributed to the lower q_p of these cells, which could result in higher relative availability of galactosylation-associated Golgi resident proteins (UDP-Gal transporter and GalT).

Despite having no observable difference in galactosylation, the intracellular profiles of UDP-Gal for 1,030 cells are different. Figure 3 shows that 1,030 A + FA8 culture has higher intracellular UDP-Gal concentration compared to the 1,030 B + FB4 culture. Because both these cultures have similar specific mAb productivities and similar levels of galactosylation, it is likely that the reduced UDP-Gal concentration in culture 1,030 B + FB4 is due to reduced biosynthesis of this nucleotide sugar and not to higher consumption. Indeed, when comparing both cultures, we see that culture 1,030 B + FB4 presents lower extracellular glucose concentration, lower specific glucose consumption rate and considerably lower extracellular Gln availability (Fig. 1C and D). Reduced intracellular UDP-Gal concentration may occur due to all these factors. Broadly, UDP-Gal is produced using two building blocks: the carbohydrate backbone (in this case glucose-derived galactose) and the nucleotide component (UTP), which is the product of pyrimidine metabolism. Low glucose availability and specific consumption would correlate with lower availability of the galactose backbone of UDP-Gal. It has been recently confirmed experimentally that differences of glucose concentration in cell culture and its consumption can affect the level of protein galactosylation (Liu et al., 2014). Similarly, low glutamine availability has been reported to negatively impact intracellular concentration of UTP (Nyberg et al., 1999). It is no coincidence that the most successful strategies in increasing UDP-Gal pools for improved recombinant protein galactosylation have relied on addition of galactose and uridine, a direct precursor of UTP (Grainger and James, 2013; Gramer et al., 2011).

Intracellular UDP-Gal concentrations are also cultivation condition-dependent for 4,384 cells. Similarly to 1,030 cells, the A + FA8 culture yields higher intracellular UDP-Gal than B + FB4 for 4,384 cells. This difference is also likely due to reduced glutamine availability and specific glucose consumption associated with the B + FB4 culture. Given the difference observed in the intracellular UDP-Gal profile, it is possible to attribute the reduction in mAb Fc glycan galactosylation to lack of UDP-Gal availability. Finally, the impact of ammonia accumulation must be discussed to confirm that reduced UDP-Gal biosynthesis is responsible for low galactosylation levels. We see that the culture with lower galactose occupancy (4,384 B + FB4) reaches a peak extracellular ammonium concentration of about 5 mM (Fig. 1G). This value is low when considering that previous publications have observed negative effects on galactosylation at extracellular ammonia concentrations above 10 mM (Borys et al., 1994; Chen and

Harcum, 2005; Gawlitzek et al., 2000), making ammonium effects unlikely and confirming that low galactose occupancy in this culture is likely dominated by low biosynthesis of UDP-Gal.

In conclusion, to the best of our knowledge this is the first study that provides an integrative understanding of cell growth, metabolism, IgG titer, and glycosylation in correlation with the dynamics of glucose and amino acid consumption when optimization of fed-batch culture such as a change in media and feed occurs. Our results demonstrate that the effect of media and process optimization on glycosylation should be understood from case to case and results from the interplay of the protein processing rate, cell metabolism, and expression and activity of Golgi resident proteins. Given the multiplicity of mechanisms involved, systems biology approaches could in the future contribute to the understanding of protein glycosylation and further aid attempts for glycoform control.

References

Ahn WS, Antoniewicz MR. 2011. Metabolic flux analysis of CHO cells at growth and non-growth phases using isotopic tracers and mass spectrometry. Metab Eng 13(5):598–609.

Ahn WS, Jeon JJ, Jeong YR, Lee SJ, Yoon SK. 2008. Effect of culture temperature on erythropoietin production and glycosylation in a perfusion culture of recombinant CHO cells. Biotechnol Bioeng 101(6): 1234–1244.

Altamirano C, Berrios J, Vergara M, Becerra S. 2013. Advances in improving mammalian cells metabolism for recombinant protein production. Electron J Biotechnol 16(3): fulltext-2.

Altamirano C, Cairo JJ, Godia F. 2001. Decoupling cell growth and product formation in Chinese hamster ovary cells through metabolic control. Biotechnol Bioeng 76(4):351–360.

Altamirano C, Illanes A, Becerra S, Cairo JJ, Godia F. 2006. Considerations on the lactate consumption by CHO cells in the presence of galactose. J Biotechnol 125(4):547–556.

Altamirano C, Paredes C, Cairo JJ, Godia F. 2000. Improvement of CHO cell culture medium formulation: Simultaneous substitution of glucose and glutamine. Biotechnol Prog 16(1):69–75.

Altamirano C, Paredes C, Illanes A, Cairo JJ, Godia F. 2004. Strategies for fed-batch cultivation of t-PA producing CHO cells: Substitution of glucose and glutamine and rational design of culture medium. J Biotechnol 110(2):171–179.

Baker KN, Rendall MH, Hills AE, Hoare M, Freedman RB, James DC. 2001. Metabolic control of recombinant protein *N*-glycan processing in NS0 and CHO cells. Biotechnol Bioeng 73(3):188–202.

Barkholt V, Jensen AL. 1989. Amino acid analysis: Determination of cysteine plus half-cystine in proteins after hydrochloric acid hydrolysis with a disulfide compound as additive. Anal Biochem 177(2):318–322.

Borys MC, Linzer DI, Papoutsakis ET. 1994. Ammonia affects the glycosylation patterns of recombinant mouse placental lactogen-I by chinese hamster ovary cells in a pH-dependent manner. Biotechnol Bioeng 43(6):505–514.

Burton DR, Dwek RA. 2006. Immunology. Sugar determines antibody activity. Science 313(5787):627–628.

Carinhas N, Duarte TM, Barreiro LC, Carrondo MJ, Alves PM, Teixeira AP. 2013. Metabolic signatures of GS-CHO cell clones associated with butyrate treatment and culture phase transition. Biotechnol Bioeng 110(12):3244–3257.

Chee Furng Wong D, Tin Kam Wong K, Tang Goh L, Kiat Heng C, Gek Sim Yap M. 2005. Impact of dynamic online fed-batch strategies on metabolism, productivity and *N*-glycosylation quality in CHO cell cultures. Biotechnol Bioeng 89(2):164–177.

Chen P, Harcum SW. 2005. Effects of amino acid additions on ammonium stressed CHO cells. J Biotechnol 117(3):277–286.

Cruz HJ, Moreira JL, Carrondo MJ. 1999. Metabolic shifts by nutrient manipulation in continuous cultures of BHK cells. Biotechnol Bioeng 66(2):104–113.

Dean J, Reddy P. 2013. Metabolic analysis of antibody producing CHO cells in fed-batch production. Biotechnol Bioeng 110(6):1735–1747.

Dorai H, Kyung YS, Ellis D, Kinney C, Lin C, Jan D, Moore G, Betenbaugh MJ. 2009. Expression of anti-apoptosis genes alters lactate metabolism of Chinese hamster ovary cells in culture. Biotechnol Bioeng 103(3): 592–608.

Druz A, Son YJ, Betenbaugh M, Shiloach J. 2013. Stable inhibition of mmu-miR-466h-5p improves apoptosis resistance and protein production in CHO cells. Metab Eng 16:87–94.

Ellgaard L, Helenius A. 2003. Quality control in the endoplasmic reticulum. Nat Rev Mol Cell Biol 4(3):181–191.

Fogolin MB, Wagner R, Etcheverrigaray M, Kratje R. 2004. Impact of temperature reduction and expression of yeast pyruvate carboxylase on hGM-CSF-producing CHO cells. J Biotechnol 109(1–2):179–191.

Fox SR, Patel UA, Yap MG, Wang DI. 2004. Maximizing interferon-gamma production by Chinese hamster ovary cells through temperature shift optimization: Experimental and modeling. Biotechnol Bioeng 85(2): 177–184.

Gagnon M, Hiller G, Luan YT, Kittredge A, DeFelice J, Drapeau D. 2011. High-end pH-controlled delivery of glucose effectively suppresses lactate accumulation in CHO fed-batch cultures. Biotechnol Bioeng 108(6): 1328–1337.

Gambhir A, Europa AF, Hu WS. 1999. Alteration of cellular metabolism by consecutive fed-batch cultures of mammalian cells. J Biosci Bioeng 87(6):805–810.

Gawlitzek M, Ryll T, Lofgren J, Sliwkowski MB. 2000. Ammonium alters *N*-glycan structures of recombinant TNFR-IgG: Degradative versus biosynthetic mechanisms. Biotechnol Bioeng 68(6):637–646.

Gonzalez-Leal IJ, Carrillo-Cocom LM, Ramirez-Medrano A, Lopez-Pacheco F, Bulnes-Abundis D, Webb-Vargas Y, Alvarez MM. 2011. Use of a Plackett-Burman statistical design to determine the effect of selected amino acids on monoclonal antibody production in CHO cells. Biotechnol Prog 27(6):1709–1717.

Goochee CF, Gramer MJ, Andersen DC, Bahr JB, Rasmussen JR. 1991. The oligosaccharides of glycoproteins: Bioprocess factors affecting oligosaccharide structure and their effect on glycoprotein properties. Biotechnology (N Y) 9(12):1347–1355.

Grainger RK, James DC. 2013. CHO cell line specific prediction and control of recombinant monoclonal antibody *N*-glycosylation. Biotechnol Bioeng 110(11):2970–2983.

Gramer MJ, Eckblad JJ, Donahue R, Brown J, Shultz C, Vickerman K, Priem P, van den Bremer ET, Gerritsen J, van Berkel PH. 2011. Modulation of antibody galactosylation through feeding of uridine, manganese chloride, and galactose. Biotechnol Bioeng 108(7):1591–1602.

Hills AE, Patel A, Boyd P, James DC. 2001. Metabolic control of recombinant monoclonal antibody *N*-glycosylation in GS-NS0 cells. Biotechnol Bioeng 75(2):239–251.

Holst B, Bruun A, Kielland-Brandt M, Winther J. 1996. Competition between folding and glycosylation in the endoplasmic reticulum. EMBO J 15(14): 3538–3546.

Hossler P, Khattak SF, Li ZJ. 2009. Optimal and consistent protein glycosylation in mammalian cell culture. Glycobiology 19(9):936–949.

Huang YM, Hu W, Rustandi E, Chang K, Yusuf-Makagiansar H, Ryll T. 2010. Maximizing productivity of CHO cell-based fed-batch culture using chemically defined media conditions and typical manufacturing equipment. Biotechnol Prog 26(5):1400–1410.

Jassal R, Jenkins N, Charlwood J, Camilleri P, Jefferis R, Lund J. 2001. Sialylation of human IgG-Fc carbohydrate by transfected rat alpha2,6-sialyltransferase. Biochem Biophys Res Commun 286(2):243–249.

Jefferis R. 2007. Antibody therapeutics: Isotype and glycoform selection. Expert Opin Biol Ther 7(9):1401–1413.

Jefferis R. 2009a. Glycosylation as a strategy to improve antibody-based therapeutics. Nat Rev Drug Discov 8(3):226–234.

Jefferis R. 2009b. Recombinant antibody therapeutics: The impact of glycosylation on mechanisms of action. Trends Pharmacol Sci 30(7): 356–362.

Jimenez Del Val I, Kontoravdi C, Nagy JM. 2010. Towards the implementation of quality by design to the production of therapeutic monoclonal antibodies with desired glycosylation patterns. Biotechnol Prog 26(6): 1505–1527.

Jimenez Del Val I, Kyriakopoulos S, Polizzi KM, Kontoravdi C. 2013. An optimized method for extraction and quantification of nucleotides and nucleotide sugars from mammalian cells. Anal Biochem 443(2): 172–180.

Jimenez Del Val I, Nagy JM, Kontoravdi C. 2011. Quantification of intracellular nucleotide sugars and formulation of a mathematical model for prediction of their metabolism. BMC Proc 5(Suppl 8):P10.

Kanda Y, Yamane-Ohnuki N, Sakai N, Yamano K, Nakano R, Inoue M, Misaka H, Iida S, Wakitani M, Konno Y, Yano K, Shitara K, Hosoi S, Satoh M. 2006. Comparison of cell lines for stable production of fucose-negative antibodies with enhanced ADCC. Biotechnol Bioeng 94(4): 680–688.

Kim SH, Lee GM. 2007. Down-regulation of lactate dehydrogenase-A by siRNAs for reduced lactic acid formation of Chinese hamster ovary cells producing thrombopoietin. Appl Microbiol Biotechnol 74(1): 152–159.

Kochanowski N, Blanchard F, Cacan R, Chirat F, Guedon E, Marc A, Goergen JL. 2008. Influence of intracellular nucleotide and nucleotide sugar contents on recombinant interferon-gamma glycosylation during batch and fed-batch cultures of CHO cells. Biotechnol Bioeng 100(4): 721–733.

Kornfeld R, Kornfeld S. 1985. Assembly of asparagine-linked oligosaccharides. Annu Rev Biochem 54:631–664.

Li J, Wong CL, Vijayasankaran N, Hudson T, Amanullah A. 2012. Feeding lactate for CHO cell culture processes: Impact on culture metabolism and performance. Biotechnol Bioeng 109(5):1173–1186.

Liu B, Spearman M, Doering J, Lattova E, Perreault H, Butler M. 2014. The availability of glucose to CHO cells affects the intracellular lipid-linked oligosaccharide distribution, site occupancy and the *N*-glycosylation profile of a monoclonal antibody. J Biotechnol 170:17–27.

Lu S, Sun X, Zhang Y. 2005. Insight into metabolism of CHO cells at low glucose concentration on the basis of the determination of intracellular metabolites. Process Biochem 40(5):1917–1921.

Mastrangelo AJ, Hardwick JM, Zou S, Betenbaugh MJ. 2000. Part II. Overexpression of bcl-2 family members enhances survival of mammalian cells in response to various culture insults. Biotechnol Bioeng 67(5):555–564.

Mori K, Kuni-Kamochi R, Yamane-Ohnuki N, Wakitani M, Yamano K, Imai H, Kanda Y, Niwa R, Iida S, Uchida K., et al. 2004. Engineering Chinese hamster ovary cells to maximize effector function of produced antibodies using FUT8 siRNA. Biotechnol Bioeng 88(7):901–908.

Mulukutla BC, Gramer M, Hu WS. 2012. On metabolic shift to lactate consumption in fed-batch culture of mammalian cells. Metab Eng 14(2):138–149.

Muthing J, Kemminer SE, Conradt HS, Sagi D, Nimtz M, Karst U, Peter-Katalinic J. 2003. Effects of buffering conditions and culture pH on production rates and glycosylation of clinical phase I anti-melanoma mouse IgG3 monoclonal antibody R24. Biotechnol Bioeng 83(3): 321–334.

Nyberg GB, Balcarcel RR, Follstad BD, Stephanopoulos G, Wang DI. 1999. Metabolic effects on recombinant interferon-gamma glycosylation in continuous culture of Chinese hamster ovary cells. Biotechnol Bioeng 62(3):336–347.

O'Callaghan PM, James DC. 2008. Systems biotechnology of mammalian cell factories. Brief Funct Genomic Proteomic 7(2):95–110.

Pacis E, Yu M, Autsen J, Bayer R, Li F. 2011. Effects of cell culture conditions on antibody N-linked glycosylation—what affects high mannose 5 glycoform. Biotechnology and Bioengineering 108(10):2348–2358.

Paulson JC, Colley KJ. 1989. Glycosyltransferases. Structure, localization, and control of cell type-specific glycosylation. J Biol Chem 264(30): 17615–17618.

Quek LE, Dietmair S, Kromer JO, Nielsen LK. 2010. Metabolic flux analysis in mammalian cell culture. Metab Eng 12(2):161–171.

Raju TS. 2003. Glycosylation variations with expression systems and their impact on biological activity of therapeutic immunoglobulins. Bioprocess Int 1:44–54.

Raju TS. 2008. Terminal sugars of Fc glycans influence antibody effector functions of IgGs. Curr Opin Immunol 20(4):471–478.

Rivinoja A, Hassinen A, Kokkonen N, Kauppila A, Kellokumpu S. 2009. Elevated Golgi pH impairs terminal *N*-glycosylation by inducing mislocalization of Golgi glycosyltransferases. J Cell Physiol 220(1): 144–154.

Schmelzer AE, Miller WM. 2002. Effects of osmoprotectant compounds on NCAM polysialylation under hyperosmotic stress and elevated pCO(2). Biotechnol Bioeng 77(4):359–368.

Sellick CA, Croxford AS, Maqsood AR, Stephens G, Westerhoff HV, Goodacre R, Dickson AJ. 2011. Metabolite profiling of recombinant CHO cells: Designing tailored feeding regimes that enhance recombinant antibody production. Biotechnol Bioeng 108(12):3025–3031.

Senger RS, Karim MN. 2003. Effect of shear stress on intrinsic CHO culture state and glycosylation of recombinant tissue-type plasminogen activator protein. Biotechnol Prog 19(4):1199–1209.

Trummer E, Fauland K, Seidinger S, Schriebl K, Lattenmayer C, Kunert R, Vorauer-Uhl K, Weik R, Borth N, Katinger H., et al. 2006. Process parameter shifting: Part I. Effect of DOT, pH, and temperature on the performance of Epo-Fc expressing CHO cells cultivated in controlled batch bioreactors. Biotechnol Bioeng 94(6):1033–1044.

Umana P, Jean-Mairet J, Moudry R, Amstutz H, Bailey JE. 1999. Engineered glycoforms of an antineuroblastoma IgG1 with optimized antibody-dependent cellular cytotoxic activity. Nat Biotechnol 17(2): 176–180.

Urlaub G, Kas E, Carothers AM, Chasin LA. 1983. Deletion of the diploid dihydrofolate reductase locus from cultured mammalian cells. Cell 33(2):405–412.

Vergara M, Becerra S, Berrios J, Osses N, Reyes J, Rodriguez-Moya M, Gonzalez R, Altamirano C. 2014. Differential effect of culture temperature and specific growth rate on CHO cell behavior in Chemostat culture. PLoS ONE 9(4):e93865.

Waldman BC, Rudnick G. 1990. UDP-GlcNAc transport across the Golgi membrane: Electroneutral exchange for dianionic UMP. Biochemistry 29(1):44–52.

Walsh G. 2003. Biopharmaceutical benchmarks—2003. Nat Biotechnol 21(8):865–870.

Walsh G. 2006. Biopharmaceutical benchmarks 2006. Nat Biotechnol 24(7): 769–776.

Walsh G. 2010. Biopharmaceutical benchmarks 2010. Nat Biotechnol 28(9): 917–924.

Weikert S, Papac D, Briggs J, Cowfer D, Tom S, Gawlitzek M, Lofgren J, Mehta S, Chisholm V, Modi N., et al. 1999. Engineering Chinese hamster ovary cells to maximize sialic acid content of recombinant glycoproteins. Nat Biotechnol 17(11):1116–1121.

Wong DC, Wong NS, Goh JS, May LM, Yap MG. 2010a. Profiling of *N*-glycosylation gene expression in CHO cell fed-batch cultures. Biotechnol Bioeng 107(3):516–528.

Wong NS, Wati L, Nissom PM, Feng HT, Lee MM, Yap MG. 2010b. An investigation of intracellular glycosylation activities in CHO cells: Effects of nucleotide sugar precursor feeding. Biotechnol Bioeng 107(2): 321–336.

Wong NSC, Yap MGS, Wang DIC. 2006. Enhancing recombinant glycoprotein sialylation through CMP-sialic acid transporter over expression in chinese hamster ovary cells. Biotechnol Bioeng 93(5): 1005–1016.

Wormald MR, Rudd PM, Harvey DJ, Chang SC, Scragg IG, Dwek RA. 1997. Variations in oligosaccharide-protein interactions in immunoglobulin G determine the site-specific glycosylation profiles and modulate the

dynamic motion of the Fc oligosaccharides. Biochemistry 36(6):1370–1380.

Yoon SK, Choi SL, Song JY, Lee GM. 2005. Effect of culture pH on erythropoietin production by Chinese hamster ovary cells grown in suspension at 32.5 and 37.0 degrees C. Biotechnol Bioeng 89(3):345–356.

Zhou M, Crawford Y, Ng D, Tung J, Pynn AF, Meier A, Yuk IH, Vijayasankaran N, Leach K, Joly J., et al. 2011. Decreasing lactate level and increasing antibody production in Chinese Hamster Ovary cells (CHO) by reducing the expression of lactate dehydrogenase and pyruvate dehydrogenase kinases. J Biotechnol 153(1–2):27–34.

Supporting Information

Additional supporting information may be found in the online version of this article at the publisher's web-site.